Design Aspects of Graphic Equalizers*

R. A. GREINER AND MICHAEL SCHOESSOW

University of Wisconsin–Madison, Department of Electrical and Computer Engineering, Madison, WI 53706, USA

The analysis and the design of graphic equalizers are discussed. Useful properties of Hurwitz polynomials and positive real functions are applied to the types of active networks commonly found in graphic equalizers. Questions concerning frequency and phase response along with the optimum number of bands and their Q are addressed, and some practical situations are examined. Seven different basic topologies are shown with a discussion of the advantages, disadvantages, and unique features of each. Three of the seven, representing the most commonly used topologies, are examined in more detail, and the important design equations for each are given. All three are shown to have minimum phase characteristics for any combination of control settings, although other performance differences exist among them.

0 INTRODUCTION

Frequency response equalizers of some type are used in almost all high-quality audio systems, mainly to compensate for room acoustics. These equalizers usually fall into the two general categories of parametric and graphic. This paper will deal only with graphic equalizers, so named because an array of narrow-band filters is normally adjusted with vertical slide controls arranged side by side to resemble a graphic display of the set frequency response [1]–[3].

Some of the many choices available in selecting or designing an equalizer are addressed, including the number of bands, the Q of the band filters, and the maximum required boost and cut. The issue of minimum phase is discussed in some detail.

Seven basic different graphic equalizer topologies are shown. Analysis techniques which are useful for filter arrays in general are presented, and their applications to the analysis of graphic equalizers are demonstrated. Overall transfer functions are derived for several designs, and the analysis techniques are used to verify minimum-phase (MP) characteristics.

A computer program is employed to verify some of the results obtained through analysis. Frequency and phase response curves for several example circuits under varying conditions of boost and cut are presented.

* Presented at the 69th Convention of the Audio Engineering Society, Los Angeles, 1981 May 12–15; revised 1982 August 9.

1 DISCUSSION

In the equalizer designs examined the Q of the individual bandpass responses was generally between 1 and 2 when the bands were adjusted for full boost or full cut (all examples were octave-band equalizers). The individual bandpass filters employed in the designs were generally second order, and in all cases except one the boost and cut capabilities of the overall circuit could be represented by mirror image families of curves. In other words, the circuits had symmetrical boost and cut characteristics. (The analysis is thus simplified since conclusions drawn concerning operation under boost conditions will also apply under cut conditions.)

The Q of a bandpass filter is given by

$$Q_0 = \frac{\omega_0}{B} = \frac{\omega_0}{\omega_2 - \omega_1} \tag{1}$$

where ω_0 is the resonance frequency, while ω_1 and ω_2 denote the −3-dB points symmetrically flanking ω_0. Eq. (1) also defines the bandwidth B. The relationship between ω_0, ω_1, and ω_2 is given by

$$\omega_0 = \sqrt{\omega_1 \omega_2} \tag{2}$$

Q_0 may now be solved for in terms of ω_1 and ω_2,

$$Q_0 = \frac{\sqrt{\omega_1 \omega_2}}{\omega_2 - \omega_1} . \tag{3}$$

For bandwidths of one octave, $\omega_2 = 2\omega_1$ and Eq. (3)

gives a value for Q_0 of about 1.4 as a starting point in an octave-band equalizer design. Similarly, for a one-third-octave per band equalizer, the value for Q_0 will be about 4.3. This procedure takes into account only the contributions of the immediately adjacent bands. For most circuit topologies the overall Q will be a function of the amount of boost or cut. In such designs the Q is typically maximum for maximum boost (or cut) and can decrease at other settings by a considerable amount depending on component values. This characteristic tends to broaden the bands and cause considerable overlap of adjacent bands for small amounts of boost or cut. Such circuits are normally designed with a high Q at maximum boost to compensate for this effect. Circuits which exhibit a higher Q characteristic for cut positions than for boost positions of the controls have appeared as well [4].

Also affecting the smoothness of adjacent band combining is the interaction between the individual filters. Although there exist circuits in which the output is simply a summation of the individual bandpass filters and a flat channel, this is not always the case. The boosting of a particular band may affect the Q or the symmetry of an adjacent band, especially in equalizer circuits which employ an overall feedback path encompassing all of the filters. This is demonstrated in the specific analyses, and is illustrated in Figs. 24–26.

Minimum phase is an often discussed characteristic concerning complex filter arrays, and it has been suggested that minimum-phase response is desirable in equalizers [5]. The response produced when a signal is passed through any minimum-phase network is one such that a second network may be constructed to recover the original signal. Except for a pure time delay, the recovered signal will be an exact replica of the original. A nonminimum-phase network will cause excessive phase lag, and to recover an exact replica of the original signal, one would require a network that violated causality and is thus not physically realizable. The output of a nonminimum-phase network may be equalized for either flat magnitude response or flat phase response, but not both. With minimum-phase networks, on the other hand, equalizing the magnitude also causes the phase to become equalized, and vice versa. Many questions remain unanswered concerning loudspeaker system and room effects on phase response. The issue of aural phase shift perception is still being debated. But regardless of one's opinion on these issues, it is useful to know whether a particular equalizer design exhibits minimum phase behavior for all combinations of control settings.

2 TOPOLOGY

Figs. 1–7 show various graphic equalizer topologies in block diagram form. Although other topologies exist, most of the designs, which have appeared commercially, are represented by one of these figures.

Referring to the figures, the slanted arrows indicate the locations of the controls in the circuits. For example, in Fig. 1, each of the filters contains the control for that band. In Fig. 2 the controls are potentiometers which pan between the two inputs at each of the summing nodes. In Fig. 5, the controls are simply output level controls from each summing node.

The seven topologies shown may be broadly divided

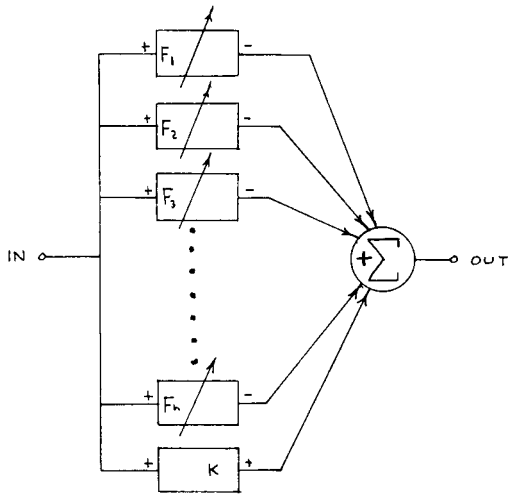

Fig. 1. Configuration for parallel-type filter. F_1, F_2, . . . are filters of the form given by Eq. (6). Band gain controls are included within each filter.

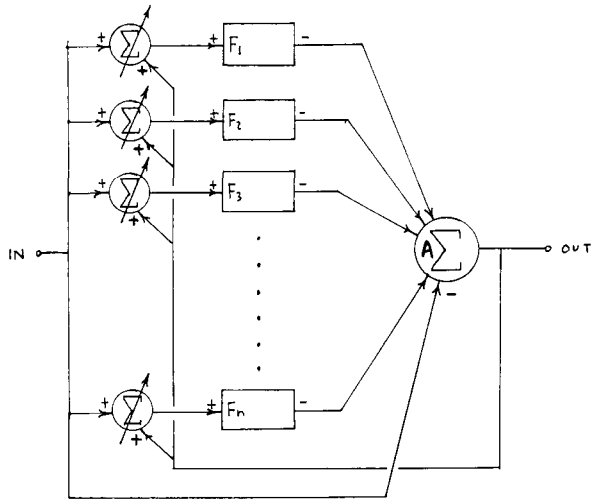

Fig. 2. Parallel-type filter using feedback summers. F_1, F_2, . . . are band-pass filters.

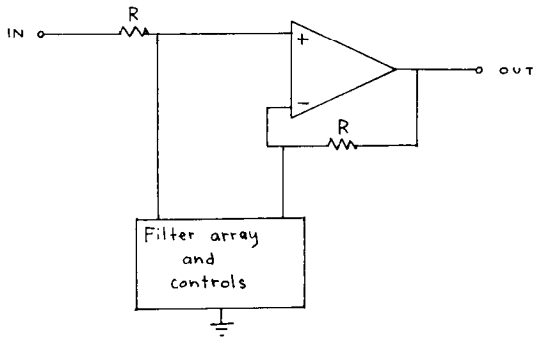

Fig. 3. In this commonly used filter configuration the filter array generally consists of passive or active resonant circuits.

into two categories: series and parallel. Fig. 6 is a series type and the other six are parallel types. In series-type equalizers, the individual filters F_i are of the type that exhibit flat response (and usually unity gain) over the audio spectrum for one position of the control. Two types of filters are commonly employed; those that can be adjusted for boost or cut, and those that can only cut (notch filters). One advantage of the series-type circuit is the ease of analysis. None of the individual filters can affect each other if they are buffered. Also, it is relatively simple to check the circuit for an overall minimum-phase characteristic since it is only required to show that the individual band filters be in general minimum phase. This may be the reason why the series-type configuration has acquired a reputation for being definitely minimum phase. The filter sections which are most often used (the RLC bridged-tee and the constant-B) are not necessarily minimum phase, as used, depending on component values. Normally bridged-tee circuits are set up such that the series and shunt resonant tank circuits are network duals, and under these conditions a minimum-phase response is obtained.

The parallel-type designs are more difficult to analyze, particularly concerning the question of minimum phase. Most of the parallel-type designs conform to one of the first three configurations (Figs. 1–3), and these three configurations will be examined in detail.

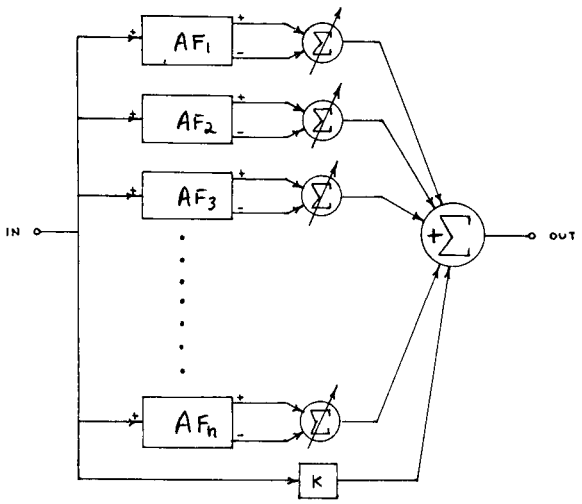

Fig. 4. F_1, F_2, . . . are band-pass filters with gain A at resonance. Positive and negative outputs are summed to provide boost and cut response.

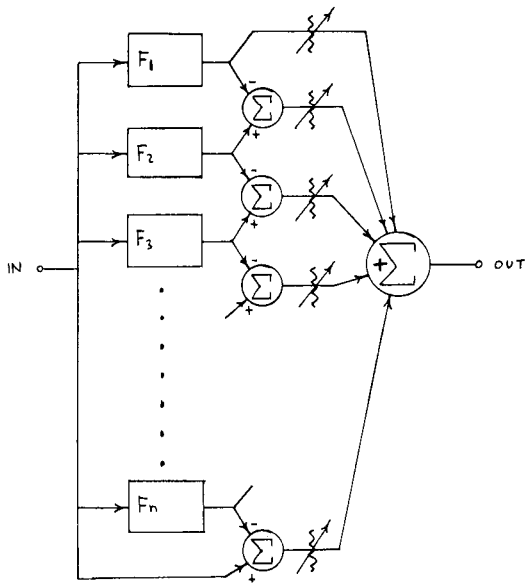

Fig. 5. F_1, F_2, . . . are low-pass filters in this arrangement where each band is created by the combination of two adjacent filters.

3 GENERAL ANALYSIS

Suppose the transfer function is known for a particular circuit. It may then be expressed in the general form

$$F(s) = \frac{A(s)}{B(s)} = \frac{E_0(s)}{E_{in}(s)} . \quad (4)$$

The stability of the circuit may be checked by plotting the poles and zeros of $F(s)$ in the s plane. If all of the poles lie in the left half-plane [the roots of $B(s)$ all have negative real parts], the circuit will be stable. Simple poles on the jω axis lead to borderline stability, while multiple poles on the jω axis represent a case of instability. The positions of the zeros [representing the roots of $A(s)$] will have no effect on stability, but for the case where they are restricted to the left half-plane, the corresponding transfer function will be of the minimum-phase variety.

Polynomials whose roots all have nonpositive real

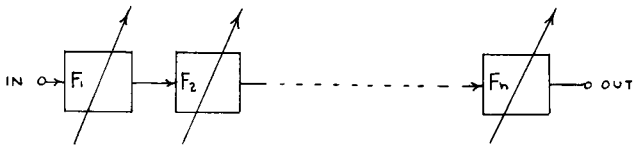

Fig. 6. Series filter set most commonly used in professional equalizing filter sets. F_1, F_2, . . . are generally notch filters or may be of the form given by Eq. (6). This is the easiest set to analyze and is usually configured to guarantee MP response.

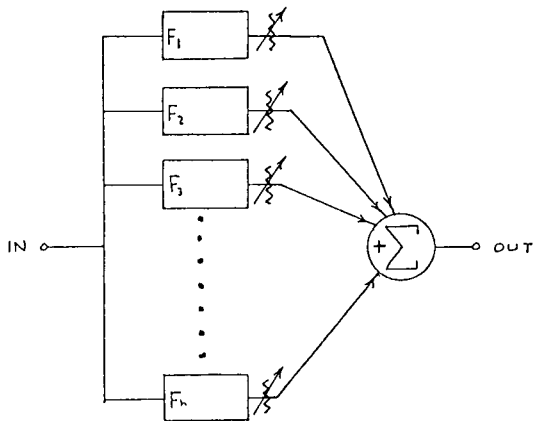

Fig. 7. The first of three filter-set topologies to be analyzed in detail. The filters are simply band-pass filters whose outputs are summed.

parts are called Hurwitz polynomials. A Hurwitz polynomial, when plotted in the s plane, will have no roots in the right half-plane and no multiple roots on the jω axis. Hurwitz polynomials with no roots on the jω axis are called "strictly Hurwitz." Several criteria exist which may be applied to polynomials to determine whether or not they are Hurwitz. The subject is covered in some detail by most texts on network synthesis and analysis [6]–[8]. In some cases it may be determined by inspection that a polynomial is not Hurwitz. For example $s^3 + 2s^2 - s + 1$ has a negative coefficient indicating at least one root with a positive real part.

The determination of Hurwitz polynomials is useful in that if the numerator $A(s)$ of a physically realizable stable transfer function $F(s) = A(s)/B(s)$ can be shown to be Hurwitz, the transfer function will be minimum phase.

Most graphic equalizer circuits have an overall transfer function which is the sum of the transfer functions of the individual band filters plus a constant. Depending on the number of bands, the overall transfer function may be quite complex. A one-third-octave (per band) design, for example, will have a transfer function with about 70 zeros. To insure minimum-phase characteristics, it must be verified that none of these reside in the right half-plane for any combination of control settings. Such verifications are seldom directly practicable, and a more efficient method of analysis is desirable.

One useful concept is that of the "positive real function." A function $G(s)$ is defined as being positive real if it satisfies the following requirements:

1) It must be a rational function in s with real coefficients.

2) It may not have poles or zeros in the right half-plane.

3) It may not have multiple poles or zeros on the jω axis.

4) It may not have the degrees of the numerator and denominator differing by more than 1.

5) It must have a nonnegative real part for all $s =$ jω.

6) It must have real and positive residues for the poles on the jω axis.

The usefulness of the positive real concept, and of Hurwitz polynomials, derives from the following properties concerning polynomials P_1 and P_2 [6]–[8]:

1) The arithmetic sum of any number of positive real functions is a positive real function.

2) All positive real transfer functions are minimum phase.

3) Any positive real transfer function P_1/P_2 may be synthesized as the driving point impedance of a two-terminal passive network ($Z_{dp} = P_1/P_2$), and conversely.

4) If and only if P_1/P_2 is positive real, then P_2/P_1 is positive real.

5) If and only if P_1 is positive real, then KP_1 is positive real, where K is a positive real number.

6) If P_1/P_2 is positive real, then P_1 and P_2 are both Hurwitz, although not necessarily vice versa.

7) If and only if P_1/P_2 are both Hurwitz, then P_1/P_2 is minimum phase and nonoscillatory.

8) If P_1 and P_2 are Hurwitz, and if one of them is also strictly Hurwitz, then P_1P_2 is Hurwitz.

9) If and only if P_1/P_2 is positive real, then $P_1 + KP_2$ is Hurwitz, where K is a positive real number.

10) A passive two-port network has a minimum-phase transfer function if there is only one transmission path connecting the input and output ports, and there are no mutual inductances.

11) A function $F(s) = K(s^2 + a_0s + a_1)/(s^2 + b_0s + b_1)$ is positive real if $a_1b_1 \geq (\sqrt{a_0} - \sqrt{b_0})^2$.

Showing that the individual band transfer functions are or are not minimum phase is fairly simple in most graphic equalizer circuits since the filters are relatively low order. With only two or three zeros whose positions must be checked, it is practical to just plot the pole–zero constellation in the s plane. If the positions of the zeros are defined in terms of component ratios, the general case may be observed.

The majority of graphic equalizer designs employ summed bandpass filters, and since the sum of several minimum-phase filters is not necessarily minimum phase, it is insufficient in these cases to simply show that each filter section is itself minimum phase. If, however, the individual band transfer functions can all be shown to be positive real, then the overall transfer function will also be positive real [property 1], and therefore minimum phase [property 2]. Of all the listed properties, property 3 is one of the most useful for quickly verifying that a particular function is positive real. Relating to this, the properties of passive driving point functions are identical to those of positive real functions.

A common design trait in graphic equalizers is for the individual band filters to have transfer functions of the form

$$F(s) = \frac{(\omega_0/Q_0)s}{s^2 + (\omega_0/Q_0)s + \omega_0^2} \qquad (5)$$

which represents a bandpass filter, or

$$F(s) = \frac{s^2 + K(\omega_0 Q_0)s + \omega_0^2}{s^2 + (\omega_0/Q_0)s + \omega_0^2}, \qquad k > 0 \qquad (6)$$

which represents a bandpass filter with unity gain in the stopband and a gain of K at resonance. Eq. (5) may be realized as the driving point function of a parallel RLC resonant circuit, thus demonstrating that it is positive real [by property 3] and minimum phase [by property 2]. Eq. (6) may be verified as positive real using properties 3) or 11). It will then also be minimum phase [property 2]. Note that higher order bandpass filters are not positive real, although they may be minimum phase.

4 SPECIFIC ANALYSIS

In Section 2, some of the more commonly used graphic equalizer topologies were illustrated. The first

three of these will be analyzed in some detail.

Configuration 1 is shown in Fig. 8 in a form useful for analysis. Each of the filters $F_i(s)$ is capable of providing symmetrical boost or cut at its center frequency, or flat response, depending on the setting of its control. A schematic representation of a single-filter section is shown in Fig. 9. For the case of full boost the potentiometer wiper is to the far left, and under these conditions the transfer function is

$$F(s) = -\frac{s^2 + s[2R_1R_2C_1 + (R_1 + R_3)(R_1 + R_2)C_2]/R_1R_2C_1C_2(R_1 + R_3) + (2R_1 + R_2)/R_1R_2C_1C_2(R_1 + R_3)}{s^2 + s[(R_1 + R_2)C_2 + 2R_2C_1 + (R_1 + R_3)C_2]/R_1R_2C_1C_2(R_1 + R_3) + (2R_1 + R_2)/R_1R_2C_1C_2(R_1 + R_3)}. \quad (7)$$

Eq. (7) is of the same form as Eq. (6), and in practice the filter can be designed to satisfy property 11). Since the overall transfer function for this design is composed of the sum of a number of such filters plus a constant, it is both positive real and minimum phase [by properties 1) and 2)]. From Fig. 8 it is seen that the summing occurs at a virtual ground point, and therefore interaction between filter sections is avoided.

Referring to Eq. (7) and Fig. 9, in practice R_3 serves only to bias the operational amplifier and is usually made much larger in value than either R_1 or R_2. Because of this, a simplification of Eq. (7) is possible. If each of the $R_1 + R_3$ terms is replaced with just R_3, the transfer function for a single filter section becomes

$$F(s) = -\frac{s^2 + s[2R_1R_2C_1 + R_3(R_1 + R_2)C_3/R_1R_2R_3C_1C_2 + (2R_1 + R_2)/R_1R_2R_3C_1C_2}{s^2 + s[(R_1 + R_2)C_2 + 2R_2C_1 + R_3C_2]/R_1R_2R_3C_1C_2 + (2R_1 + R_2)/R_1R_2R_3C_1C_2}. \quad (8)$$

The equations may now be written for center frequency ω_0 and $Q_{0\,\max}$.

$$\omega_0 = \sqrt{\frac{2R_1 + R_2}{R_1R_2R_3C_1C_2}} \quad (9)$$

$$Q_{0\,\max} = \sqrt{\frac{2R_1 + R_2}{R_1R_2R_3C_1C_2}} \times \frac{R_2R_3C_1C_2}{(R_1 + R_2)C_2 + 2R_2C_1 + R_3C_2}. \quad (10)$$

These equations are inconvenient to work with as they appear and a simplification is desirable. A useful procedure is to specify ratios for some components. A ratio of $C_1 = 10C_2$ broadly optimizes Q_0, and $R_3 = 10R_2$ is reasonable for reasons previously mentioned. Eqs. (9) and (10) may then be reduced to

$$\omega_0 = \frac{1}{10R_2C_2}\sqrt{2 + \frac{R_2}{R_1}} \quad (11)$$

$$Q_{0\,\max} = \sqrt{\frac{2R_1 + R_2}{9.6R_1}}. \quad (12)$$

The equation for passband gain A_0 [which is equal to the ratio of the s term coefficients in Eq. (8)] appears in simplified form as

$$A_{0\,\max} = -\left(\frac{9.6Q_0^2 - 2}{3} + 1\right). \quad (13)$$

Eqs. (11)–(13) are used to design the filter sections.

At a glance it may appear that $A_{0\,\max}$ and $Q_{0\,\max}$ can be chosen independently. Unfortunately this is not true. For any chosen value of $A_{0\,\max}$, there is only one value of $Q_{0\,\max}$ possible. For example, if $A_{0\,\max}$ is set at 4 (or 12-dB maximum boost and cut), the value of $Q_{0\,\max}$ is 1.1. As it turns out, 1.1 is not a bad value for $Q_{0\,\max}$ if six to ten bands are to be used in the overall design. This circuit, however, cannot be used for larger designs such as half-octave or third-octave where it is desirable to have $Q_{0\,\max}$ values between 2.5 and 5. Going back to Eqs. (9) and (10) with different ratios for C_1, C_2 and R_2, R_3 does not significantly alter the situation. Q_0 decreases from its maximum value for conditions other than full boost or full cut. This is illustrated in Fig. 21(b).

Once the individual filters are designed, the remaining resistor values in Fig. 8 may be calculated. The overall transfer function is

$$\frac{E_0(s)}{E_{in}(s)} = -\frac{R_f}{R_a} + \frac{R_f}{R_b}(\Sigma_i F_i(s)). \quad (14)$$

If we wish to generate an overall transfer function

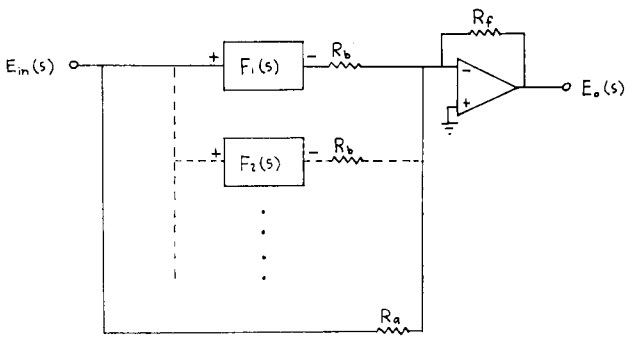

Fig. 8. This realization of the filter topology of Fig. 9 is used for analysis. Each filter is capable of providing a symmetrical boost or cut at its center frequency.

which is flat in frequency response, that is,

$$\frac{E_0(s)}{E_{in}(s)} = A \ , \tag{15}$$

and with the conditions that all controls are centered, we find

$$A = -\frac{R_f}{R_a} + n\frac{R_f}{R_b} \tag{16}$$

where n is the number of bands. For the special case of one filter section, $F_1(s)$, set at full boost with all others set flat, we can write

$$\frac{E_0}{E_{in}} = -\frac{R_f}{R_a} + (n-1)\frac{R_f}{R_b} + \frac{R_f}{R_b}F_1(s) \equiv \frac{R_f}{R_b}F_1(s) \ . \tag{17}$$

This implies

$$-\frac{R_f}{R_a} + (n-1)\frac{R_f}{R_b} = 0 \tag{18}$$

which yields

$$R_a = \frac{R_b}{n-1} \ . \tag{19}$$

Note that R_f falls out of the equation as expected, since it simply represents a gain multiplier. Its value can be found from Eq. (16), where it specifies the flat response circuit gain. The magnitudes of R_a and R_b are important only in the sense that their ratio must be the correct value.

Configuration 2 is shown in Fig. 10 in a form useful for analysis. The individual band filters $F_1(s)$ are second-order bandpass filters of the form

$$F(s) = -\frac{(\omega_0/Q_0)s}{s^2 + (\omega_0/Q_0)s + \omega_0^2} \ . \tag{20}$$

When potentiometer R_1 in Fig. 10 is adjusted with its wiper to the far left, the frequency band covered by $F_1(s)$ is accentuated in the overall circuit output. Positioning the wiper of R_1 to the far right causes a large amount of negative feedback to occur at this same frequency, thus causing attenuation in the forward signal path. In each case the remaining filters $F_i(s)$ receive percentages of both the input signal $E_{in}(s)$ and the output signal $E_0(s)$ in ratios determined by their respective potentiometer settings.

From Fig. 10 the overall transfer function may be derived:

$$E_0(s) = -[E_{in}(s) + E_x(s)] \tag{21}$$

$$E_0(s) = -E_{in}(s) - A\,\Sigma_i\, E_i F_i(s) \tag{22}$$

where

$$E_i(s) = (1 - x_i)E_{in}(s) + x_i E_0(s) \ . \tag{23}$$

Then

$$-E_0(s) = E_{in}(s) + A\,\Sigma_i\,[(1 - x_i)E_{in}(s) + x_i E_0(s)]F_i(s) \ . \tag{24}$$

The general form of the overall transfer function is then

$$\frac{E_0}{E_{in}(s)} = -\frac{1 + A\,\Sigma_i\,(1 - x_i)F_i(s)}{1 + A\,\Sigma_i\,x_i F_i(s)} \ . \tag{25}$$

The effects of various settings of the potentiometers may now be investigated. For the special case with all of the controls centered, x will be equal to 0.5 for each band. Eq. (25) then yields $E_0(s)/E_{in}(s) = -1$, as expected. For the special case with band 1 set for full boost ($x_1 = 0$) and all other bands set flat ($x = 0.5$),

$$\frac{E_0(s)}{E_{in}(s)} = -\left[1 + \frac{AF_1(s)}{1 + 0.5A\sum_{i=2}^{n} F_i(s)}\right] \tag{26}$$

and for band 1 at full cut ($x_1 = 1$) with all other bands flat we have

$$\frac{E_0(s)}{E_{in}(s)} = -\left[1 + \frac{AF_1(s)}{1 + 0.5A\sum_{i=2}^{n} F_i(s)}\right]^{-1} \tag{27}$$

where A is defined as R_b/R_a in Fig. 10.

At this point some approximations are appropriate. For an array of second-order bandpass filters $F_i(s)$ which satisfies Eqs. (1) and (2) in terms of frequency spacing and Q, we can write

$$\sum_{i=1}^{\infty} F_i(s) \approx K \tag{28}$$

where K is a constant representing the average value of the complete summation. This is illustrated in Fig. 11. When Eq. (3) is satisfied, K is approximately 1.2–1.3. For finite larger groups of filters the approximation remains useful near the center of the frequency range covered by the group. Fig. 12 illustrates the summation of nine filters, as would be the case for an octave band equalizer. From Eq. (28) it follows that

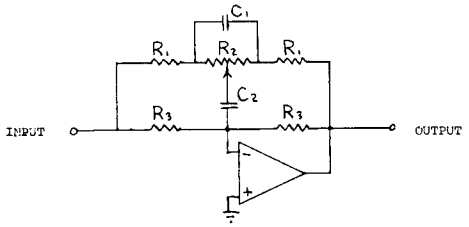

Fig. 9. Schematic of each filter section used in the configuration of Fig. 8.

$$\sum_{i=2}^{\infty} F_i(s) = \sum_{i=1}^{\infty} F_i(s) - F_1(s) \approx K - F_1(s) \quad (29)$$

where $F_1(s)$ is the response of one filter section alone. If the frequency band described by $F_1(s)$ resides near the center of a large but finite group of filters, Eq. (28) may be applied with suitably altered limits. Eq. (29) is used to eliminate the $F_i(s)$ term in Eq. (26). With $K = 1.2$ we have

$$\frac{E_0(s)}{E_{in}(s)} \approx -\left[1 + \frac{AF_1(s)}{1 + 0.5A(1.2 - F_1(s))}\right]. \quad (30)$$

Replacing $F_1(s)$ with the general form for a bandpass filter [as given in Eq. (20)],

$$\frac{E_0(s)}{E_{in}(s)} \approx -\frac{s^2 + [(1 + 1.1A)/(1 + 0.6A)]\,(\omega_0/Q_0)s + \omega_0^2}{s^2 + [(1 + 0.1A)/(1 + 0.6A)]\,(\omega_0/Q_0)s + \omega_0^2}. \quad (31)$$

Eq. (31) describes the same special case as Eq. (26), that is, all bands set flat except for one (the one centered at ω_0 in this case) fully boosted. Eq. (31) yields the following information concerning the response with a single fully boosted band [or a fully cut band considering the symmetry between Eqs. (26) and (27)]. With a single band set for full boost or full cut and all other bands set flat, the gain at the center frequency of the boosted band will be

$$A_v\Big|_{\omega=\omega_0} \approx \frac{1 + 1.1A}{1 + 0.1A} \quad (32)$$

and the Q will be

$$Q_{max} \approx Q_0 \frac{1 + 0.6A}{1 + 0.1A}. \quad (33)$$

To investigate how Q varies with differing amounts of boost or cut the appropriate values of x_1 may be put into Eq. (25) and the corresponding succeeding equations again derived.

For any combination of control settings Eq. (25) will have the form of a fraction in which the numerator and denominator each consist of the sum of a group of positive real functions plus unity [assuming the bandpass filters $F_i(s)$ are of the form of Eq. (20)]. Therefore the numerator and denominator are both themselves positive real functions [properties 1) and 5)], and the form of Eq. (25) is

$$\frac{E_0(s)}{E_{in}(s)} = -\frac{P_1(s)/P_2(s)}{P_3(s)/P_2(s)} \quad (34)$$

where $P_1(s)$, $P_2(s)$, and $P_3(s)$ are polynomials. Since $-P_1(s)/P_2(s)$ and $P_3(s)/P_2(s)$ are both positive real functions, it follows that $P_1(s)$, $P_2(s)$, and $P_3(s)$ are all Hurwitz polynomials [property 6)]. Eq. (34) reduces to the ratio of two Hurwitz polynomials, and thus describes a minimum-phase function [property 7)], verifying that the overall response curve for this equalizer

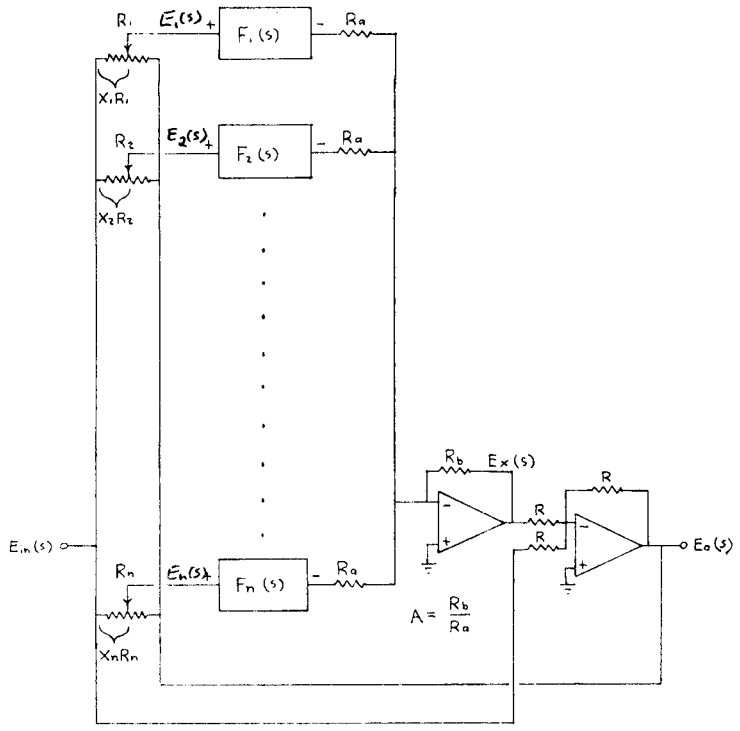

Fig. 10. The second of the three configurations discussed in detail. Each filter is a second-order band-pass circuit of the form given by Eq. (20).

topology will always be minimum phase.

The topology most widely used in graphic equalizers is the one represented by configuration 3 and shown in more detail in Fig. 13. The series RLC resonant filters are labeled Z_1, Z_2, Z_3, etc. They each provide a low-impedance path to ground at their particular resonant frequency. If the wiper of potentiometer R_1 in Fig. 13 is moved to the far left, a high-loss voltage divider will exist in the forward signal path at frequency F_1. Positioning the wiper to the far right will effect a high feedback loss, causing a corresponding boost in the forward signal path. The effects introduced by the various potentiometer settings are not entirely independent since the individual resonant circuits are not isolated by buffer amplifiers or virtual ground-driving points.

For the special case with only a single filter section (Fig. 14) we have, for the transfer function,

$$\frac{E_0(s)}{E_{in}(s)} = \frac{s^2 + s(R_3R_4 + R_2R_4 + R_2R_3 + R_1R_2)/L(R_2 + R_3) + 1/LC}{s^2 + s(R_3R_4 + R_2R_4 + R_2R_3 + R_1R_3)/L(R_2 + R_3) + 1/LC} . \quad (35)$$

This is of the same form as Eq. (6), and in practice can be made to satisfy property 11). From Eq. (35) it is seen that

$$\omega_0 = \sqrt{\frac{1}{LC}} \quad (36)$$

$$Q_0 = \sqrt{\frac{L}{C}} \frac{R_2 + R_3}{R_3R_4 + R_2R_4 + R_2R_3 + R_1R_3} . \quad (37)$$

For the case of full boost ($R_3 = 0$ in Fig. 14), the transfer function reduces to

$$\frac{E_0(s)}{E_{in}(s)} = \frac{s^2 + s(R_1 + R_4)/L + 1/LC}{s^2 + s(R_4/L) + 1/LC} . \quad (38)$$

Under these conditions,

$$Q_{0\,max} = \frac{1}{R_4}\sqrt{\frac{L}{C}} \quad (39)$$

$$A_{0\,max} = \frac{R_1 + R_4}{R_4} . \quad (40)$$

From Eqs. (37) and (39) it can be seen that this is a circuit for which the Q is highest under conditions of full boost or full cut. The amount of Q reduction for midway settings of the control is largely determined by the values of R_2 and R_3, which represent the potentiometer. Typical values of $Q_{0\,max}$ range from 1.5 to 2.0. Eq. (40) shows that after R_4 is chosen for a particular

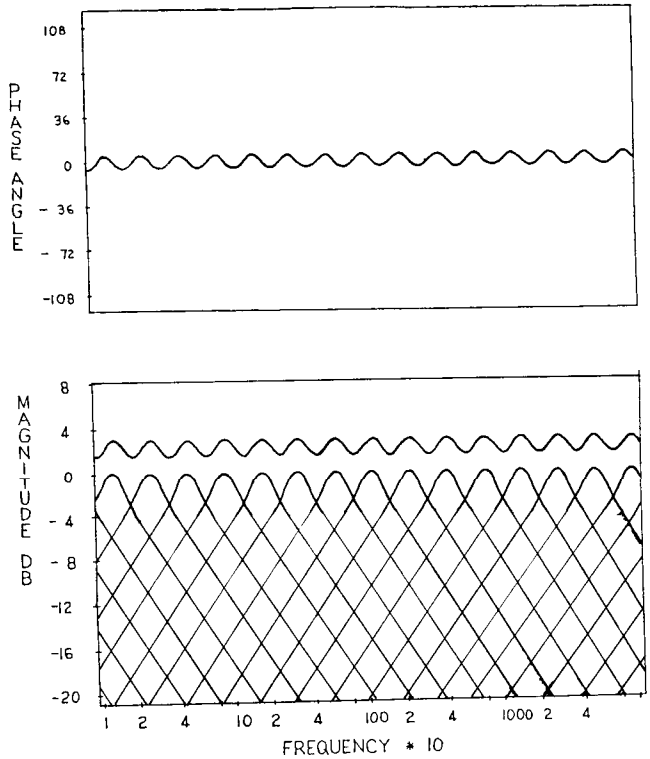

Fig. 11. Magnitude and phase responses for the filter array of Fig. 10. Only the summed response is shown for the phase angle.

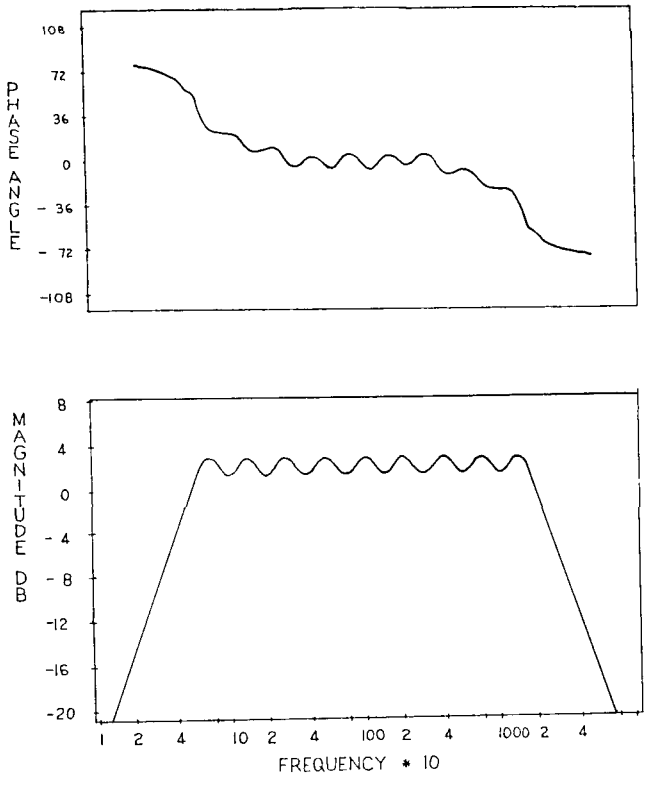

Fig. 12. For a finite group of filter sections, nine in this case, the phase and amplitude response curves show considerably more band end variation. Compare this to Fig. 11.

value of $Q_{0\ max}$, the maximum obtainable boost and cut is set by R_1. The effective contours of the controls, relative to gain and Q, are dependent on the potentiometer values. Values which are large compared to R_4 in Fig. 14 will cause most of the control range to be near the extremes, with little variation for settings near the middle. Large potentiometer values will also cause the Q of the bands to be somewhat lower for any given setting except full boost or full cut, and the variation of Q with boost will become greater. Note that $Q_{0\ max}$ will not be affected. In practice it is desirable to reduce the Q variation by making the potentiometers low resistance compared to R_4. There exists, however, a practical lower limit on the potentiometer values because of the resulting decreased loop gain for the operational amplifier. This may result in a significant reduction in high-frequency accuracy or dc stability. One design solution is to put an additional gain stage inside the feedback loop. Alternatively two or three complete circuits may be connected in series and the controls distributed evenly among them. Then each of the two or three operational amplifiers would be required to drive only one-half or one-third as many potentiometers in its feedback network.

It has been shown that the circuit transfer function is minimum phase for the case with only a single filter. For the more general case, with a large number of filter sections, direct nodal analysis is not practicable, and a different approach is required in checking for an overall minimum-phase characteristic. The circuit can be redrawn as in Fig. 15. If a wye–delta transformation is performed on each filter section as shown in Fig. 16, the circuit in Fig. 15 can be transformed to that of Fig. 17. The parallel combination of all the Z_d is represented by Z_d' and similarly for Z_e' and Z_f'. Nodal analysis of the circuit in Fig. 17 gives

$$\frac{E_0}{E_{in}} = \frac{1 + R/Z_e'}{1 + R/Z_d'} = \frac{(Z_e' + R)/Z_e'}{(Z_d' + R)/Z_d'} . \qquad (41)$$

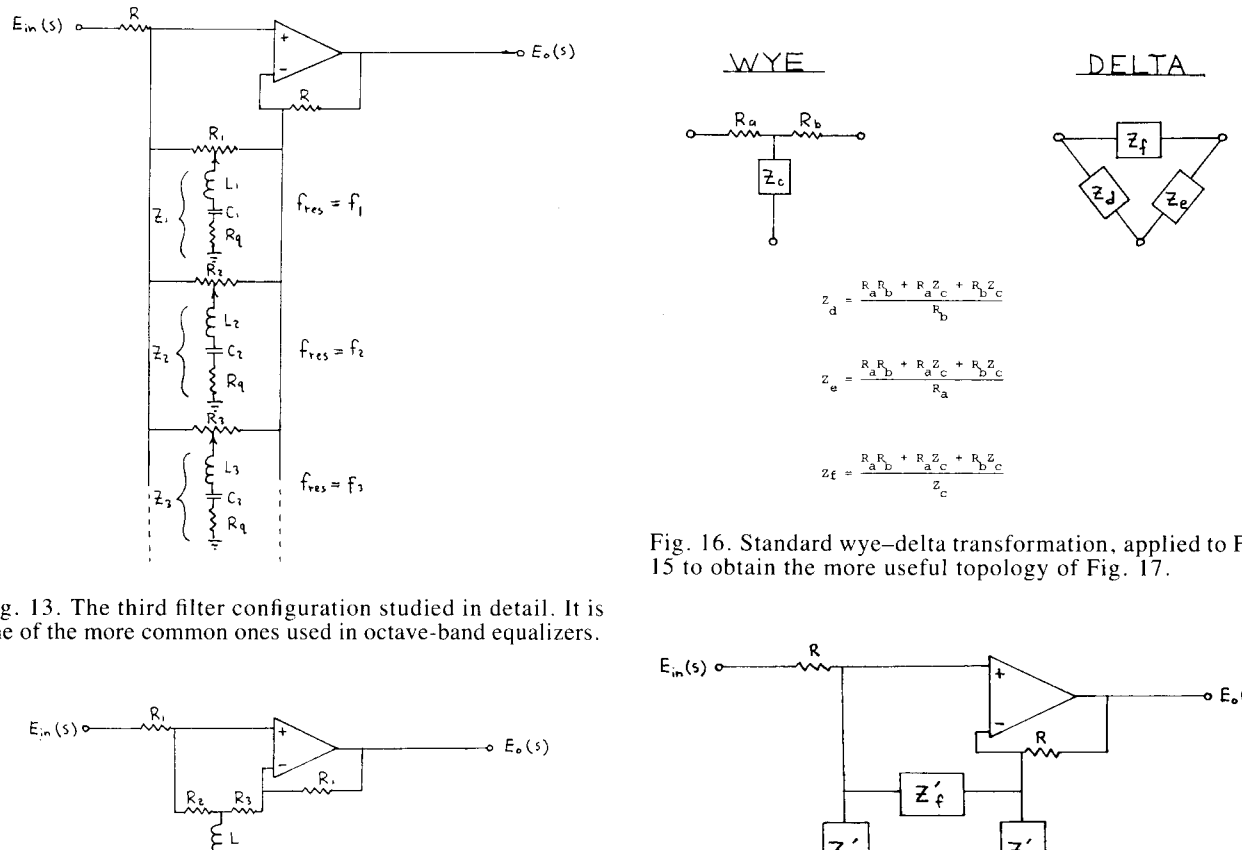

Fig. 15. This representation of the filter set of Fig. 13 is used as the basis of the transformation described in detail.

Fig. 16. Standard wye–delta transformation, applied to Fig. 15 to obtain the more useful topology of Fig. 17.

Fig. 17. Transformed topology of the original circuit of Fig. 13. It can now be readily analyzed to give Eq. (41).

Fig. 13. The third filter configuration studied in detail. It is one of the more common ones used in octave-band equalizers.

Fig. 14. This single section of the filter set of Fig. 13 is used to derive Eq. (35).

As expected, Z_f' does not appear in the equation since it is connected across the input terminals of an operational amplifier. Note that when $Z_d' = Z_e'$, which occurs when all the controls are set to the center, the circuit gain is unity.

From Fig. 16 the form of the individual Z_d and Z_e is found to be

$$Z = \frac{s^2LC + sRC + 1}{sC} . \quad (42)$$

This function can be synthesized as the driving-point impedance of a series RLC network. Functions Z_d' and Z_e' can be synthesized as parallel combinations of such networks as shown in Fig. 18 and are therefore positive real functions.

Since we know that Z_f' is effectively out of the circuit, it may be eliminated from the schematic. What remains is essentially a pair of filter circuits connected in series as shown in Fig. 19. The transfer function of filter 1 is

$$T_1 = \frac{Z_d'}{Z_d' + R} = \frac{1}{1 + R/Z_d'} . \quad (43)$$

The transfer function of filter 2 is

$$T_2 = \frac{Z_e' + R}{Z_e'} . \quad (44)$$

Note that the product of the functions T_1T_2 equals E_0/E_{in}, as in Eq. (41). Referring to Eq. (43), Z_d' is known to be positive real so R/Z_d' is also positive real by properties 4) and 5). The quantity $1 + R/Z_d'$ is positive real by property 1), and therefore Eq. (43) as a whole is positive real by property 4). A similar line of reasoning shows Eq. (44) to be positive real as well. It is concluded that filters 1 and 2 in Fig. 19 are both minimum-phase types. Since two or more minimum-phase filters connected in series have an overall transfer function that is minimum phase, it has now been shown that this particular graphic equalizer topology is in fact minimum phase, for any combination of settings.

Practical designs utilizing this circuit usually replace the RLC branches with RC electronic equivalents, as shown in Fig. 20. The driving-point impedance for Fig. 20(a) is

$$Z_{dp} = \frac{s^2LC + sRC + 1}{s} \quad (45)$$

while that for Fig. 20(b) is

$$Z_{dp} = \frac{s^2(R_1^2 + R_1R_2)C_1C_2 + s(R_1C_1) + 1}{sC_1} . \quad (46)$$

The new equations for center frequency and Q_{0max}, referring to Fig. 20(b), are

$$\omega_0 = \sqrt{\frac{1}{(R_1^2 + R_1R_2)C_1C_2}} \quad (47)$$

$$Q_{0\,max} = \sqrt{\frac{(R_1 + R_2)C_2}{R_1C_1}} . \quad (48)$$

Each of the configurations examined has been shown to have minimum-phase characteristics for any combination of control settings. Configuration 1 also has an overall transfer function which is positive real, although this does not appear to have any practical significance. Configurations 2 and 3 exhibit adjacent band amplitude interaction while configuration 1 does not. The choice of topologies may also depend upon the cost and complexity of construction. In this area, configuration 3 appears the most attractive.

The performance of all three configurations was also examined with the aid of a computer, using an electronic circuit analysis program (ECAP). Various combinations of control settings were implemented for each of the circuits, with the resulting magnitude and phase plots shown in Figs. 21–29. In each case, nine bands were employed, spaced at one-octave intervals, and with the center section at 1 kHz. These are numbered, one through nine, low-frequency to high-frequency band, for reference in the figures.

Configuration 1 (see Figs. 8 and 9):
$R_1 = 10$ kΩ, $R_2 = 100$ kΩ, $R_3 = 1$ MΩ, $C_1 = 10C_2$. Maximum boost or cut for a single band is 12 dB. $Q_{0\,max} \cong 1.1$.

Configuration 2 (see Fig. 10):
F_i are inverting, two-pole bandpass filters. Maximum boost or cut for a single band is 12 dB. Q_0 of $F_i \cong 1.4$. Q of overall circuit (with one band fully boosted) $\cong 3$.

Configuration 3 (see Fig. 13):
$R = 3$ kΩ. Potentiometers = 5 kΩ. Maximum boost or cut for a single band is 12 dB. $Q_{0\,max} \cong 1.7$.

The component values used in the ECAP programs were similar to those commonly found in commercial units.

The significant differences between the three configurations are displayed in the figures.

Circuit 1 with its relative low band Q produces broad but very smooth composite curves. The lack of adjacent band interference in this design is seen when comparing it to circuit 3 (comparing Figs. 24 and 26), where such effects act to further increase the gain when several adjacent sections are boosted.

The variation of Q with boost differs considerably in the three circuits and is shown in Figs. 21, 22, and 23.

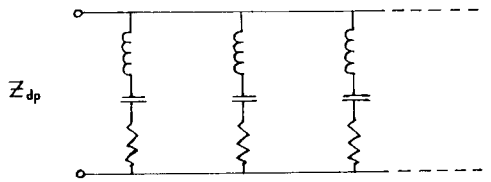

Fig. 18. Parallel resonant circuits as shown are positive real type.

Configuration 2 displays several effects, the mechanism of which may not be immediately apparent. Although the individual bandpass filters have Q_0 of 1.4, the overall circuit displays a much higher single band Q. This is due to the output signal of the overall circuit being fed back out of phase to the adjacent bands, where it subtracts from the skirt regions of the boosted band, thus effectively increasing its Q. Note that when several adjacent bands are boosted, the skirt-subtracting phenomenon operates only on the outsides of the end bands in the group. In effect then, one can have a low Q band flanked by higher Q bands, and by suitable adjustment of the controls obtain a relatively flat plateau with sharp cutoff on each side (Fig. 25). As the Q_0 the bandpass filters is increased, the skirt-subtracting effect is reduced due to the increasing ratio of band spacing to bandwidth. Unfortunately, high Q combined with one-octave spacing between bands will leave gaps such that a narrow (one octave wide, for example) boost will not be possible for many frequencies. One solution to this problem, which has been used commercially, is to make the individual filters adjustable in frequency. Reducing the Q_0 of the filters to a very low value initially (say, 0.5–1.0) is not practical, since the skirt-subtracting effect begins to dominate, even in the passband. For example, if the Q_0 of the filters is set at 0.7, it is necessary to set R_f/R_a (Fig. 10) to 200 in order to obtain 12 dB of boost. Stopband ripple also becomes excessive under these conditions. Another characteristic of this design, not shared with the other two, is asymmetrical boost and cut curves for bands near the edge of the group.

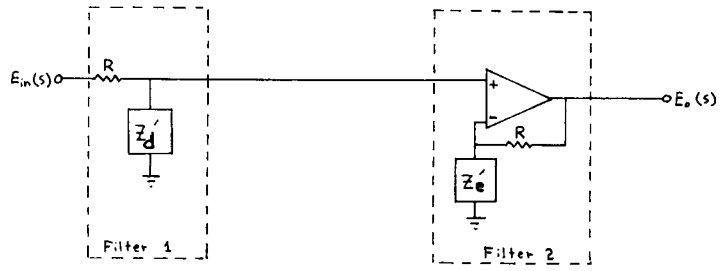

Fig. 19. This essentially simple connection of the transformed circuit of Fig. 13 shows that the overall circuit is MP.

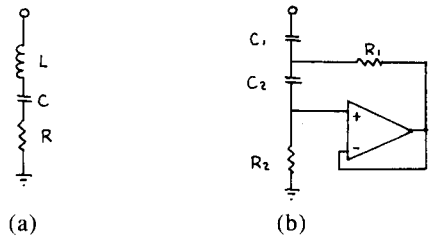

Fig. 20. The circuit shown in (a) is often replaced with the electronic equivalent (b). In either case the filter remains MP.

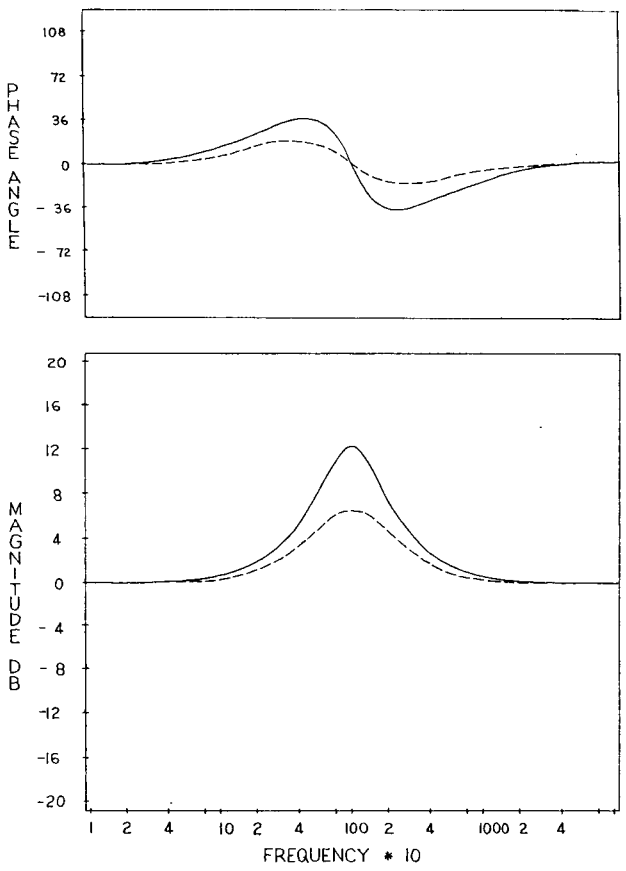

Fig. 21. Configuration 1 with band 5 set at +6 dB (dashed) and +12 dB (solid), and all other bands set flat.

5 CONCLUSION

Analysis techniques have been demonstrated which can be used to derive overall transfer functions for graphic equalizers, and to verify whether or not a particular topology exhibits minimum-phase characteristics at all times. Derivation of overall Q and boost/cut range were also demonstrated.

It was shown that three of the more common topologies exhibit minimum-phase characteristics for any combination of control settings, although differences in Q and band interaction exist among them. These results were verified with a computer analysis.

We have not addressed the questions of the audible significance of minimum-phase performance nor of the minimum-phase characteristics of loudspeakers. Higher order and narrow-band filters remain to be evaluated, however. These are not commonly used in home-lis-

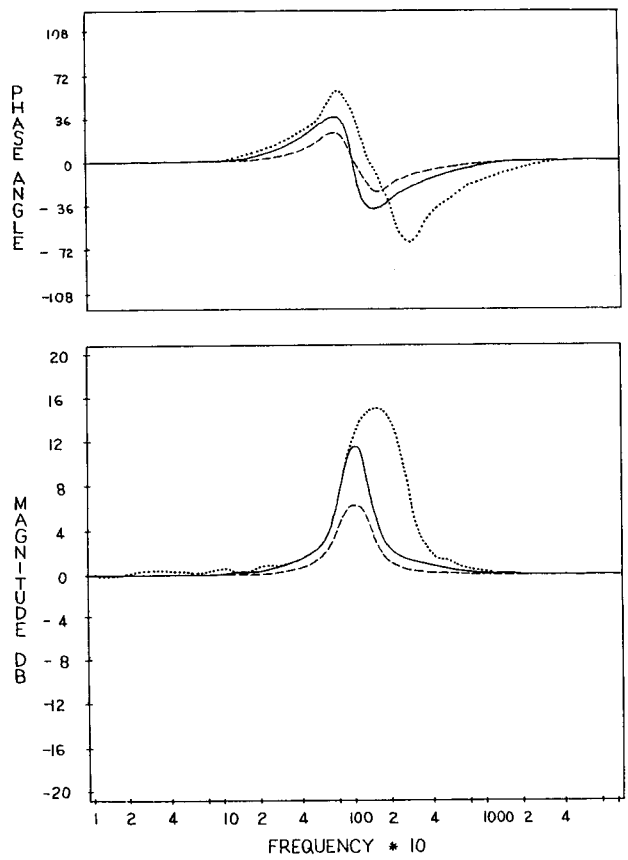

Fig. 22. Configuration 2 with band 5 set at +6 dB (dashed) and +12 dB (solid), and all other bands set flat. The dotted line shows bands 5 and 6 both set to +12 dB.

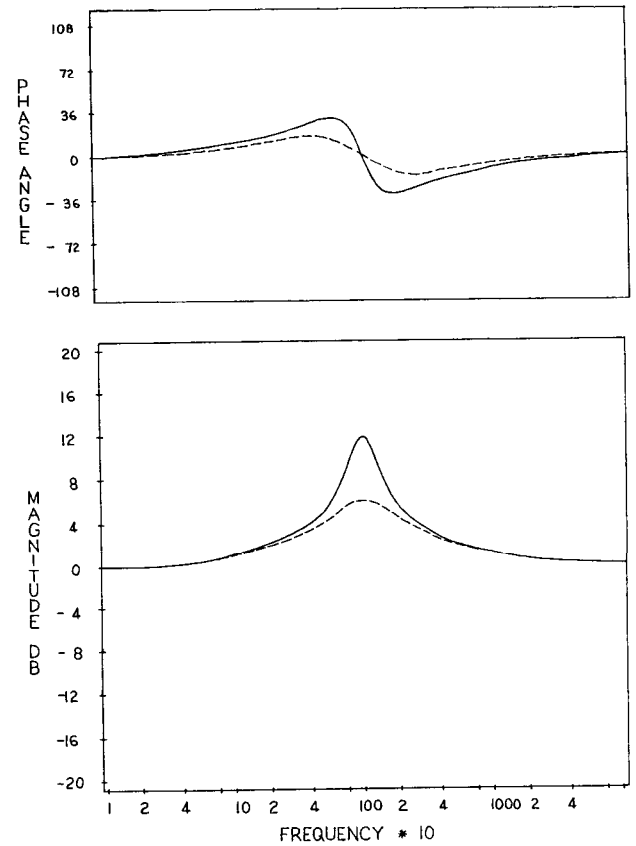

Fig. 23. Configuration 3 with band 5 set at +6 dB (dashed) and +12 dB (solid), and all other bands set flat.

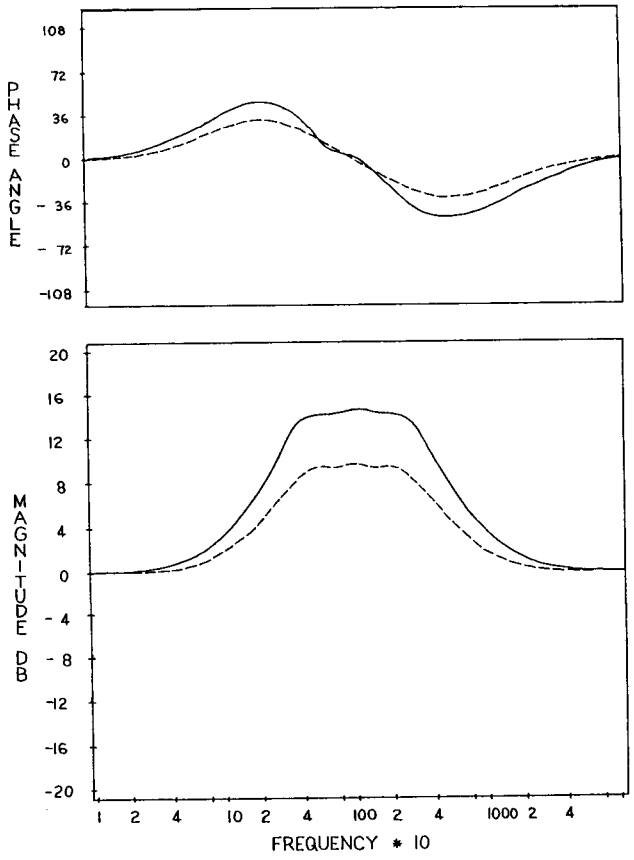

Fig. 24. Configuration 1 with bands 4, 5, and 6 each set at +6 dB (dashed) and +12 dB (solid), and all other bands set flat.

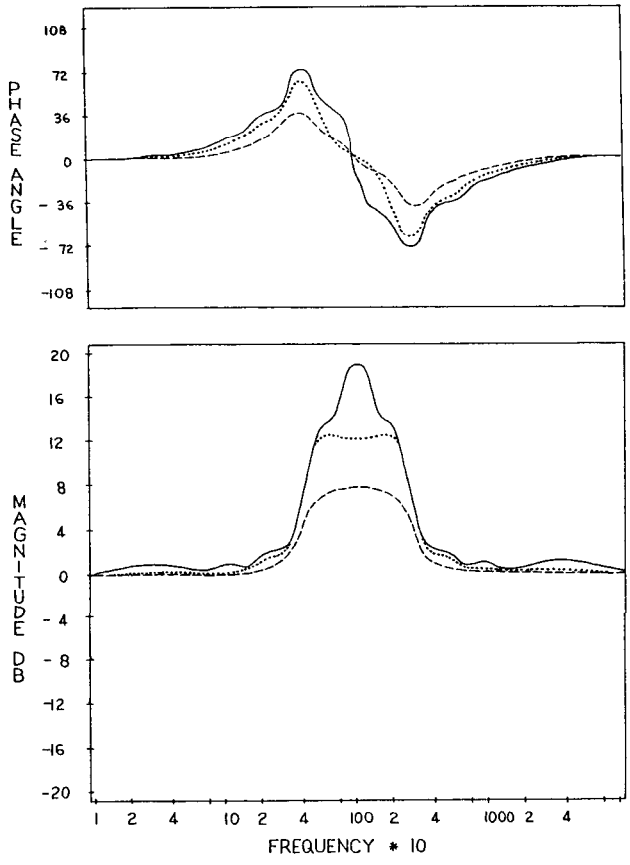

Fig. 25. Configuration 2 with bands 4, 5, and 6 each set at +6 dB (dashed) and +12 dB (solid), and all other bands set flat. The dotted line shows bands 4 and 6 set at +12 dB, while band 5 is adjusted for a flat plateau.

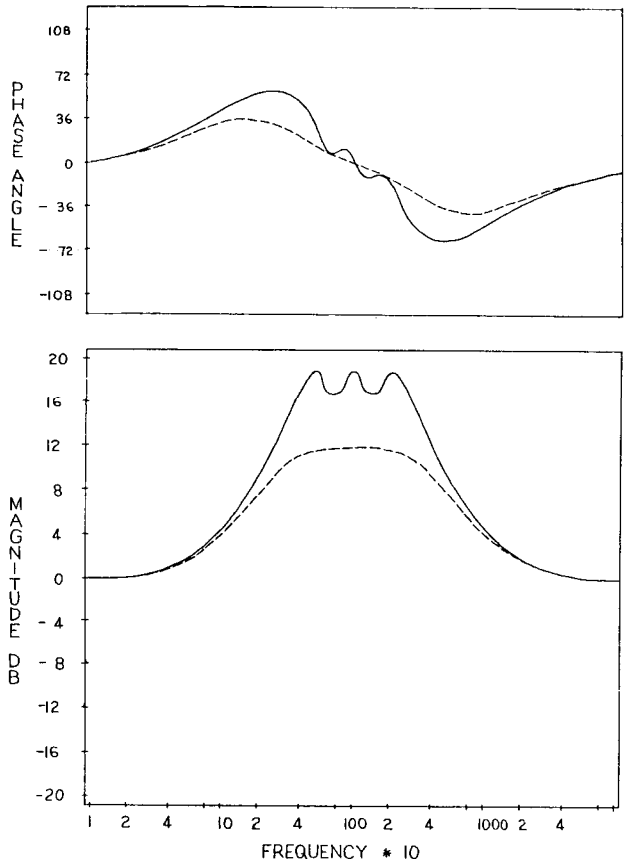

Fig. 26. Configuration 3 with bands 4, 5, and 6 each set at +6 dB (dashed) and +12 dB (solid), and all other bands set flat.

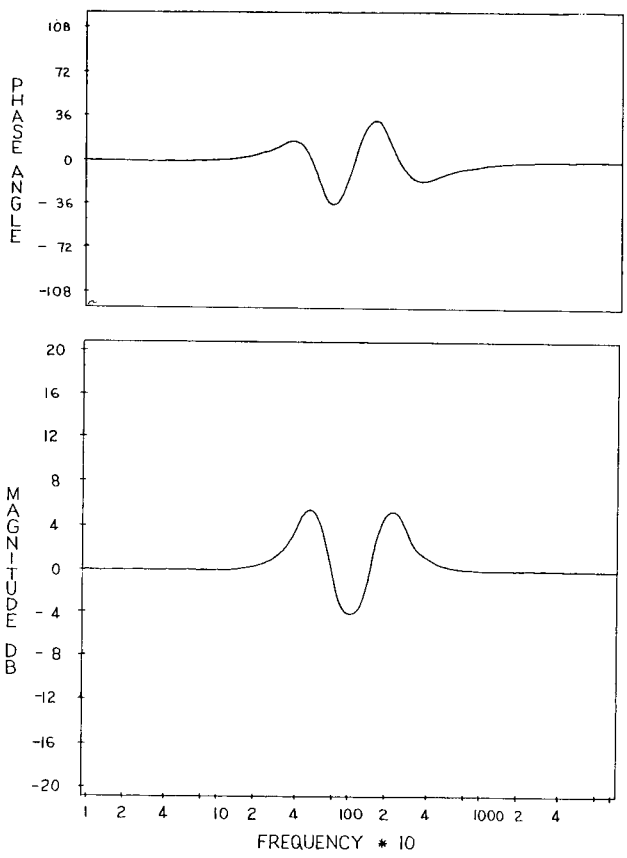

Fig. 28. Configuration 2 with bands 4, 5, and 6 set at +6 dB, −6 dB, and +6 dB, respectively, and all other bands set flat.

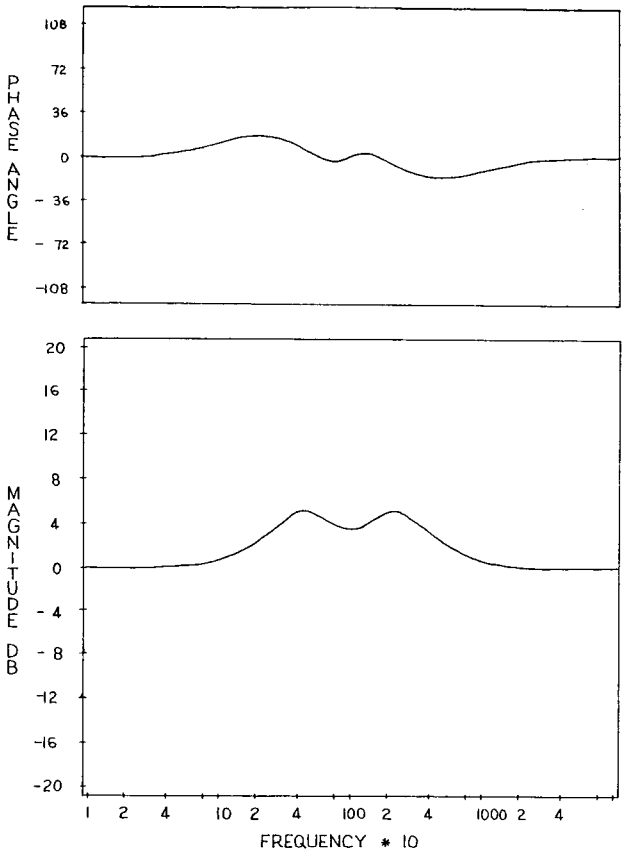

Fig. 27. Configuration 1 with bands 4, 5, and 6 set at +6 dB, −6 dB, and +6 dB, respectively, and all other bands set flat.

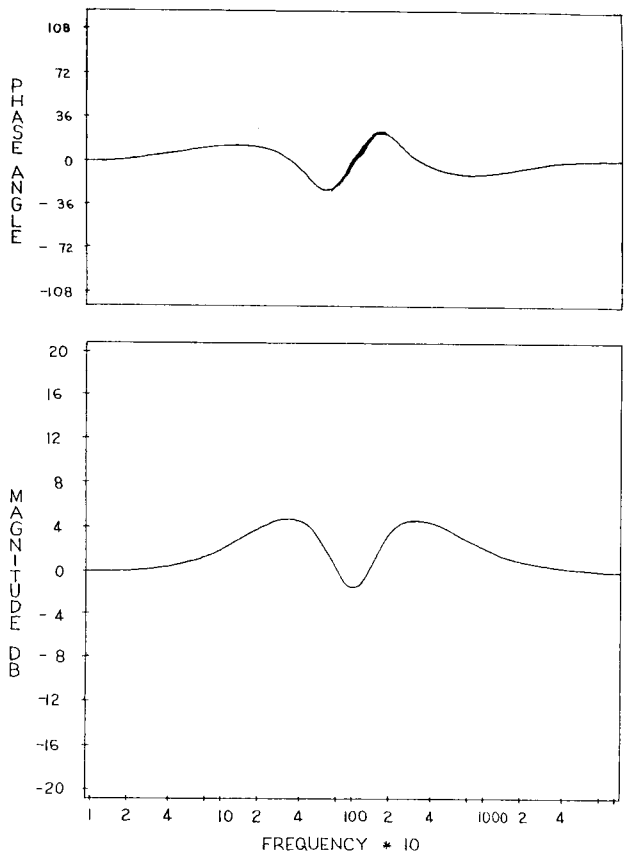

Fig. 29. Configuration 3 with bands 4, 5, and 6 set at +6 dB, −6 dB, and +6 dB, respectively, and all other bands set flat.

tening systems, but are employed mainly in the equalization of auditoriums where other criteria are preeminent.

6 REFERENCES

[1] D. N. Flickinger, "Electronic Adjustment of Monitoring Acoustics," *J. Audio Eng. Soc.*, vol. 18, pp. 657–661 (1970 Dec.).

[2] D. Queen, "Equalization of Sound Reinforcement Systems," *Audio*, p. 18 (1972 Nov.).

[3] R. F. Allison, "The Loudspeaker/Living Room System," *Audio* (1971 Nov.).

[4] J. Gorin, "Graphic Equalizer for Your Stereo System," *Radio Electronics*, p. 37 (1978 May).

[5] G. Stanley, "Minimum Phase: Defined and Illustrated," *Tech. Topics, Synergetic Audio Concepts*, vol. 5, no. 10 (1978 Apr.).

[6] S. S. Haykin, *Active Network Theory* (Addison-Wesley, Reading, MA, 1970).

[7] G. Daryanani, *Principles of Active Network Synthesis and Design* (Wiley, New York, 1976).

[8] L. Weinberg, *Network Analysis and Synthesis* (McGraw-Hill, New York, 1962).

[9] *Audio Handbook* (National Semiconductor Corp., 1976).

APPENDIX

TRANSFER FUNCTIONS AND PERFORMANCE DATA FOR CIRCUITS 4, 5, 6, AND 7

The overall transfer function for configuration 4 (see Fig. 4) is

$$\frac{E_0(s)}{E_{in}(s)} = K + A \sum_{i=1}^{n} F_i(s)(2X_i - 1) . \quad (49)$$

In a practical circuit the controls are potentiometers which pan between the inverting and noninverting outputs of the filters. In Eq. (49) X represents the potentiometer setting. For flat response, $X = 0.5$ for each band, while $X = 1$ represents full boost and $X = 0$ represents full cut. The constant K is normally set to 1. The value of A determines the maximum available boost and cut.

A disadvantage of this topology is that the boost and cut curves will not be mirror image complements. While the full boost curves are represented by Eq. (6) [assuming $F_i(s)$ are second-order bandpass filters], the full cut curves resemble notch filters of the form

$$F(s) = \frac{s^2 + \omega_0^2}{s^2 + \omega_0/Q_0 + \omega_0^2} . \quad (50)$$

The circuit configuration is in general minimum phase for suitably chosen filters $F(s)$ (second-order bandpass filters, for example), and has the advantage of independently selectable Q and gain ratios in the bands.

A somewhat more parts-efficient topology eliminates the inverters in each bandpass filter and uses instead one inverter common to all bands placed at the input of the main summing node.

The overall transfer function for configuration 5 (see Fig. 5) is

$$\frac{E_0(s)}{E_{in}(s)} = K_1F_1(s) + K_{n+1}[1 - F_n(s)] + \sum_{i=2}^{n-1} K_i[F_i(s) - F_{i-1}(s)] \quad (51)$$

where K is a measure of the voltage gain through the attentuators. For flat response all of the controls are set at $K = 0.25$ (assuming a desired boost and cut capability of 12 dB). Full boost is effected in a particular band by setting its control for no attenuation ($K = 1$). A gain of $K = 0.0625$ results in a 12-dB cut. Note that for overall unity gain with all controls set flat, a 12-dB gain output buffer is required.

This circuit requires the summed outputs of the band filters to add a constant whenever they are all set at equal levels. Because of this the Q and the spacing of the filters are critical if flat response is to be ensured when all controls are set to their flat response positions. This represents a disadvantage of the design.

For overall minimum-phase response, the low-pass filters must be first order, which will result in the output being a summation of second-order bandpass filters plus one low-pass filter and one high-pass filter.

The overall transfer function for configuration 6 (see Fig. 6) is

$$\frac{E_0(s)}{E_{in}(s)} = F_1(s)F_2(s) \cdots F_n(s) . \quad (52)$$

This configuration has the unique advantage that for an overall minimum-phase response, the necessary and sufficient condition is that the individual filters $F(s)$ be minimum phase. This advantage is very attractive when designing a one-third-octave or a one-sixth-octave unit.

The overall transfer function for configuration 7 (see Fig. 7) is

$$\frac{E_0(s)}{E_{in}(s)} = \sum_{i=1}^{n} K_i F_i(s) \quad (53)$$

where K is a measure of the voltage gain through the attenuators. For flat response all of the controls are set at $K = 0.25$ (assuming a desired boost and cut capability of 12 dB). Full boost and full cut are effected by setting $K = 1$ and $K = 0.0625$, respectively. As with configuration 5, the Q and the frequency spacing of the filters are critical if flat response is desired when all controls are at the same relative positions.

For overall minimum-phase response at all settings the bandpass filters must be second order, and for overall unity gain with all controls in the flat position, a 12-dB gain output buffer is required.

The biographies of R. A. Greiner and Michael Schoessow were published in the March issue.